J Toxicol Pathol 2024; 37: 207–212

Short Communication

Immunohistochemical characteristics of cytokeratin expression in epithelial type thymoma and thymic epithelial hyperplasia in F344 rats

Yuki Tomonari[1*], Junko Sato[1], Mitsutoshi Uchida[1], Takeshi Kanno[1], Takuya Doi[1], and Yoshiyasu Kobayashi[2]

[1] Pathology Department, Kashima Laboratories, Non-clinical Business Segment, Mediford Corporation, Kamisu-shi, Ibaraki 314-0255, Japan
[2] Department of Veterinary Medicine, Obihiro University of Agriculture and Veterinary Medicine, Nishi 2-11 Inada-cho, Obihiro, Hokkaido 080-8555, Japan

Abstract: We have previously reported on thymomas in Wistar Hannover rats with medullary differentiation and revealed that two different cytokeratin (CK) immunohistochemical types of thymic epithelia (TE), CK18 and CK14, lead to the formation of cortical-medullary structures. In aged F344 rats, epithelial-type thymoma rarely occurs, and thymic epithelial hyperplasia is common. However, CK expression in these F344 rat lesions is unknown. We investigated three hyperplasia and four thymomas in F344 for histopathological features and CK18 and CK14 expression. Hyperplasia was characterized by an increase in tubular structures in the medulla. Thymomas were nodular in shape, with tubular structures similar to those observed in hyperplasia, along with irregular structures such as cord, papillary, and spindloid. Immunohistochemical analysis revealed that the tubular structures consisted of two layers: inner cuboidal-to-columnar TE and outer round-to-oval TE, positive for CK18 and CK14, respectively. The two-layer pattern was maintained to some extent in the irregular structures. (DOI: 10.1293/tox.2024-0045; J Toxicol Pathol 2024; 37: 207–212)

Key words: epithelial type thymoma, epithelial hyperplasia, F344 rat, immunohistochemistry, CK14, CK18

Rat thymomas have been described to vary from those with or without medullary differentiation; furthermore, the latter have variable proportions of neoplastic epithelial cells and lymphocytes between tumors and within a given tumor according to the International Harmonization of Nomenclature and Diagnostic criteria (INHAND)[1]. Thymomas in rodents are categorized into epithelial and spindeloid types according to the proportion and/or features of the neoplastic epithelia[1]. The pleomorphic variations in thymic epithelial hyperplasia (TE hyperplasia) are similar to the spectrum of cellular forms of thymomas[2]. Therefore, the distinction between thymoma and TE hyperplasia is based on the size of the proliferative area[1, 2].

We previously reported that almost all thymomas in Wistar Hannover (WH) rats show medullary differentiation[3] and revealed that two different CK immunohistochemical types of thymic epithelia lead to the formation of cortical-medullary structures[4]. Cytokeratin (CK) 18-positive epithelia formed a cortex-like lymphocyte-rich area and CK 14-positive epithelia formed a medullary differentiation area, suggesting that the proliferation of different-types of thymic epithelia (TE) would form cortical-medullary structures. In contrast, in aged F344 rats, epithelial-type thymoma without medullary differentiation rarely occurs, while TE hyperplasia is common[2, 5]. Characteristics of TE hyperplasia include increased cords and tubules within the lobules, whereas those of epithelial thymoma include a focal expansile mass of tubules[1]. Moore *et al.* reported an incidence of 0.16% (277/175,136) in their extensive study on thymomas in F344/N rats, with predominant histopathological characteristics including epithelial proliferation with cord/tubule, spindloid and papillary patterns[6]. In this study, we investigated how CK18 expressed in the cortex and CK14 expressed in the medullary epithelia of WH rats might be expressed in TE hyperplasia and epithelial-type thymoma of F344 rats. Additionally, we explored the relationship between TE hyperplasia and epithelial-type thymomas.

TE hyperplasia in one male and two females (Case No. 1–3) and epithelial-type thymomas in three males and one females (Case No. 4–7) were examined histopathologically and immunohistochemically. In the background carcino-

Received: 2 May 2024, Accepted: 2 July 2024
Published online in J-STAGE: 25 July 2024
*Corresponding author: Y Tomonari
(e-mail: yuki.tomonari@mediford.com)
(Supplementary material: refer to PMC https://www.ncbi.nlm.nih.gov/pmc/journals/1592/)

genicity studies (104-week period, 400 males and 399 females, 1988–2016) including Case No. 1–7, the incidence of TE hyperplasia were 20.3% in males and 34.3% in females, and the incidence of epithelial-type thymomas were 0.8% in males and 0.3% in females.

The animals were cared for and euthanized according to the principles outlined in the Guidelines for the Care and Use of Laboratory Animals by the Japanese Association of Laboratory Animal Science and the guidelines of our institution. Thymuses collected at necropsy were fixed in 10% phosphate-buffered formalin for 1 month, embedded in paraffin, and sectioned at a thickness of 4 μm for light microscopic examination. Hematoxylin and eosin (HE) and Periodic acid-Schiff (PAS) staining were performed according to standard methods. Thymomas are categorized as epithelial and spindeloid types by INHAND for rodents[1]. However, we specifically examined the detailed features of TE hyperplasia and thymomas by referring to the criteria reported by Moore *et al.*, which included tubular, cord, papillary, and spindloid growth structures[6]. The maximum lengths of the major and minor axes of each lesion were calculated on whole-slide images using a digital pathology whole-slide scanner and software (Aperio AT2, S. No. 7277, Aperio eSlide Manager, Leica Microsystems GmbH, Wetzlar, Germany). The paraffin sections were analyzed immunohistochemically using antibodies against CK18 (Mouse monoclonal, Ks18.04, PROGEN Biotechnik, Heidelberg, Germany), CK14 (Rabbit monoclonal, ab181595, Abcam, Cambridge, UK), and α-SMA (Anti-alpha Smooth Muscle Actin: Rabbit polyclonal, ab5694, Abcam). Polymer kits were used as secondary antibodies (Histofine Simple Stain Rat MAX PO(MULTI), Code: 414191, NICHIREI BIOSCIENCE INC., Tokyo, Japan for CK18 and α-SMA; Histofine Simple Stain AP(MULTI), Code: 414261, NICHIREI BIOSCIENCE INC., for CK14). 3,3′-diaminobenzidine (liquid DAB+ substrate chromogen system, Code: K3467, Agilent Technologies, Santa Clara, CA, USA) for CK18 and α-SMA and New Fuchsin substrate kit (Code: 415161, NICHIREI BIOSCIENCE INC.) for CK14 were used to visualize the target antigens[7, 8]. The procedures and primary antibodies used for immunohistochemical examinations are shown in Table 1. To assess the staining patterns of CK18 and CK14, each positively stained area in thymoma was synthesized into a section image of Case No. 5 by image analysis platform HALO® (Indica Labs Inc., Albuquerque, NM, USA). CK18-positive areas are visualized in red, and CK14-positive areas in yellow. The areas that stained positive for CK18 and CK14 are indicated in orange. The negative areas are indicated in blue.

The histopathological findings are summarized in Table 2. TE hyperplasia was characterized by a massive increase in tubular and cord structures in the medulla of the atrophic thymus, but the expansion was limited within the thymic lobule, being less than 1.9 mm (major axis) × 0.8 mm (minor axis) (Fig. 1A). The tubular structure was lined with cuboidal-to-columnar TE with basally located nuclei showing no pleomorphism (Fig. 2A). Some thymic lymphocytes were observed in areas of TE hyperplasia (Fig. 2A).

In thymomas, proliferating TE formed an extremely enlarged nodule that exceeded the size of a thymic lobule and grew to more than 2.7 mm (major axis) × 2.1 mm (minor axis) (Fig. 1C, 1E). In addition to the tubular structures, cord, papillary, and spindloid structures were observed (Fig. 2D, 2G, 2J, and 2M). The tubular structure resembled that of TE hyperplasia, consisting of cuboidal-to-columnar TE with basally located nuclei showing some pleomorphism. Many of these tubular structures were larger and more distorted than those in TE hyperplasia, and some lumina of the tubules were indistinct (Fig. 2D). The cord structure was TE lined up into ribbons (Fig. 2G), the papillary structure was TE bending and protruding into the lumen (Fig. 2J), and the spindloid structure was composed of compact nests of proliferative round-to-oval TE forming sheets and swirls (Fig. 2M). Few lymphocytes were observed in the area of TE proliferation.

In normal thymus, epithelial cells are immunohistochemically positive for CK18 in the cortex and CK14 in the medulla and subcapsular area[4]. In the present study, immunohistochemical investigations revealed that the tubular structures consisted of luminal cells surrounded by another layer of round-to-oval cells in both the TE hyperplasia and thymomas of F344 rats. The inner and outer layers were clearly identified by the different CK types of TE. In the tubular structures of TE hyperplasia, the inner TE layer was positive for CK18 (Fig. 2B), and the outer TE layer was positive for CK14 (Fig. 2C). In thymomas, the two-layer pattern of TE was maintained in the tubular structures (Fig. 2E, 2F) and was irregularly present even in regions where there were no obvious luminal structures such as the cord (Fig. 2H, 2I) and papillary structures (Fig. 2K, 2 L). In

Table 1. The Procedures and Primary Antibodies Used for Immunohistochemical Examination

Antibody	Supplier	Cat. No.	Lot. No.	Host	Clone	Dilution	Antigen retrieval
CK18 [Ks18.04]	PROGEN Biochami	61028	603141	Mouse	Monoclonal	×8,000	Protease (NICHIREI BIOSCIENCE.INC., Code: 415231, Lot No. H1711), Hot plate 37°C, 10 min
CK14 [EPR17350]	abcam	ab181595	GR 200352-25	Rabbit	Monoclonal	×4,000	Antigen retrieval solution pH9 (NICHIREI BIOSCIENCE. INC., Code: 415211, Lot No. H2106), Autoclave 121°C, 5 min
α-SMA	abcam	ab5694	GR 3183259-33	Rabbit	Polyclonal	×1,000	Not done

Table 2. Histopathological Findings of Hyperplasia and Thymoma

	Case No.	Sex	Size (μm) major × minor axes	Growth structure	Two-layer pattern	PAS-positive material	Basement membrane
Hyperplasia	1	Male	1,417 × 749	Tubular Cord	Present Irregular but present	Present (few) Absent	Present Irregular but present
	2	Female	1,826 × 194	Tubular	Present	Present	Present
	3	Female	1,635 × 353	Tubular	Present	Present	Present
Thymoma	4	Male	5,646 × 2,736	Tubular	Present	Irregular but present	Irregular but present
	5	Male	3,335 × 2,647	Tubular Cord	Irregular but present Irregular but present	Irregular but present Absent	Irregular but present Irregular but present
	6	Male	2,751 × 2,118	Tubular Papillary Spindloid	Present Irregular but present Absent	Irregular but present Absent Absent	Irregular but present Irregular but present Irregular but present
	7	Female	4,749 × 2,842	Tubular Cord Spindloid	Present Irregular but present Absent	Irregular but present Absent Absent	Irregular but present Irregular but present Irregular but present

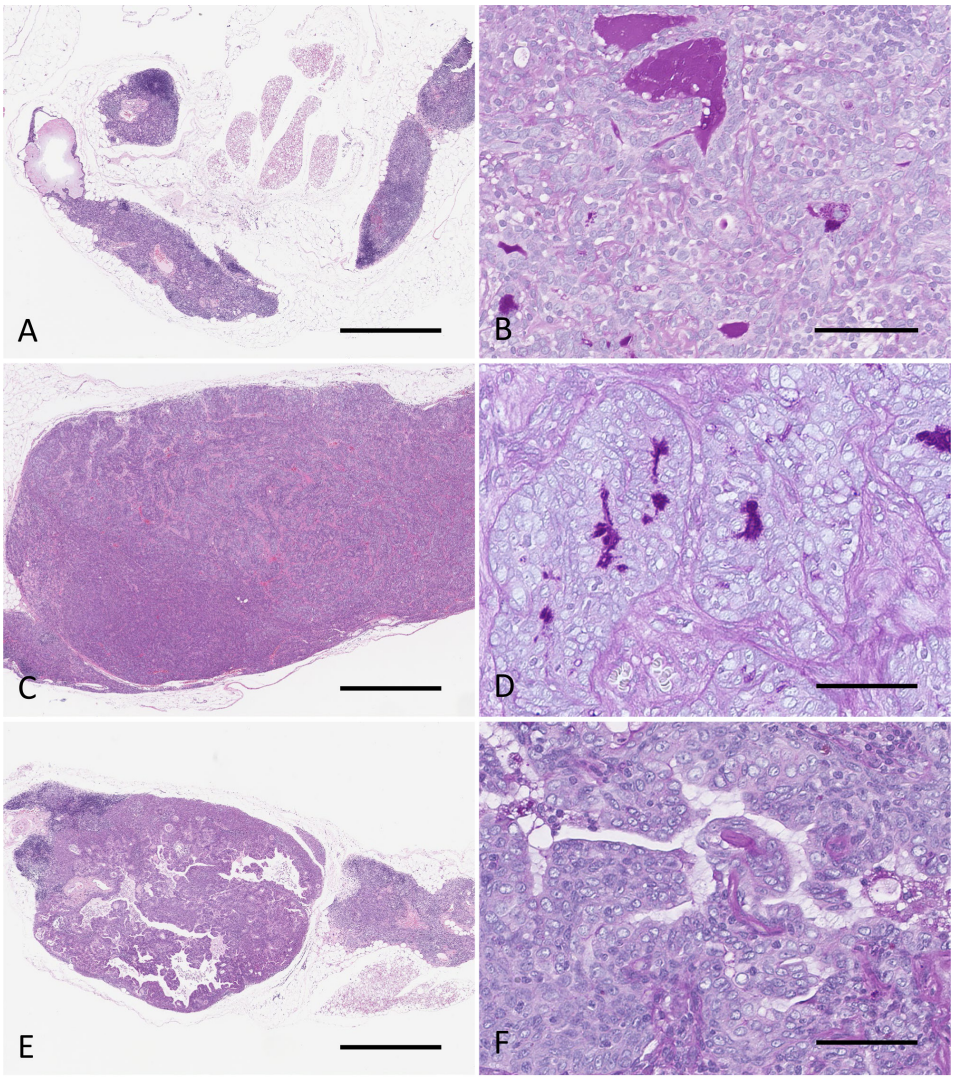

Fig. 1. A and B: TE hyperplasia, Case No. 3. C and D: Thymoma, Case No. 4. E and F: Thymoma, Case No. 6. In the TE hyperplasia, there is an increase in the tubular structures at the medulla and growth expansion limited within the lobules of the thymus (A), BM surrounds the tubules and PAS-positive material in the lumens (B). In thymomas, there is an extremely enlarged nodule including proliferating tubular structures (C), with BM surrounding tubules and PAS-positive materials in the lumens (D), an enlarged nodule including tubular and papillary structures (E), with irregularly stained BM and absence of PAS-positive material (F). A, C, and E: Hematoxylin and Eosin, Bar=1 mm. B, D, and F: Periodic acid-Schiff stain, Bar=60 μm.

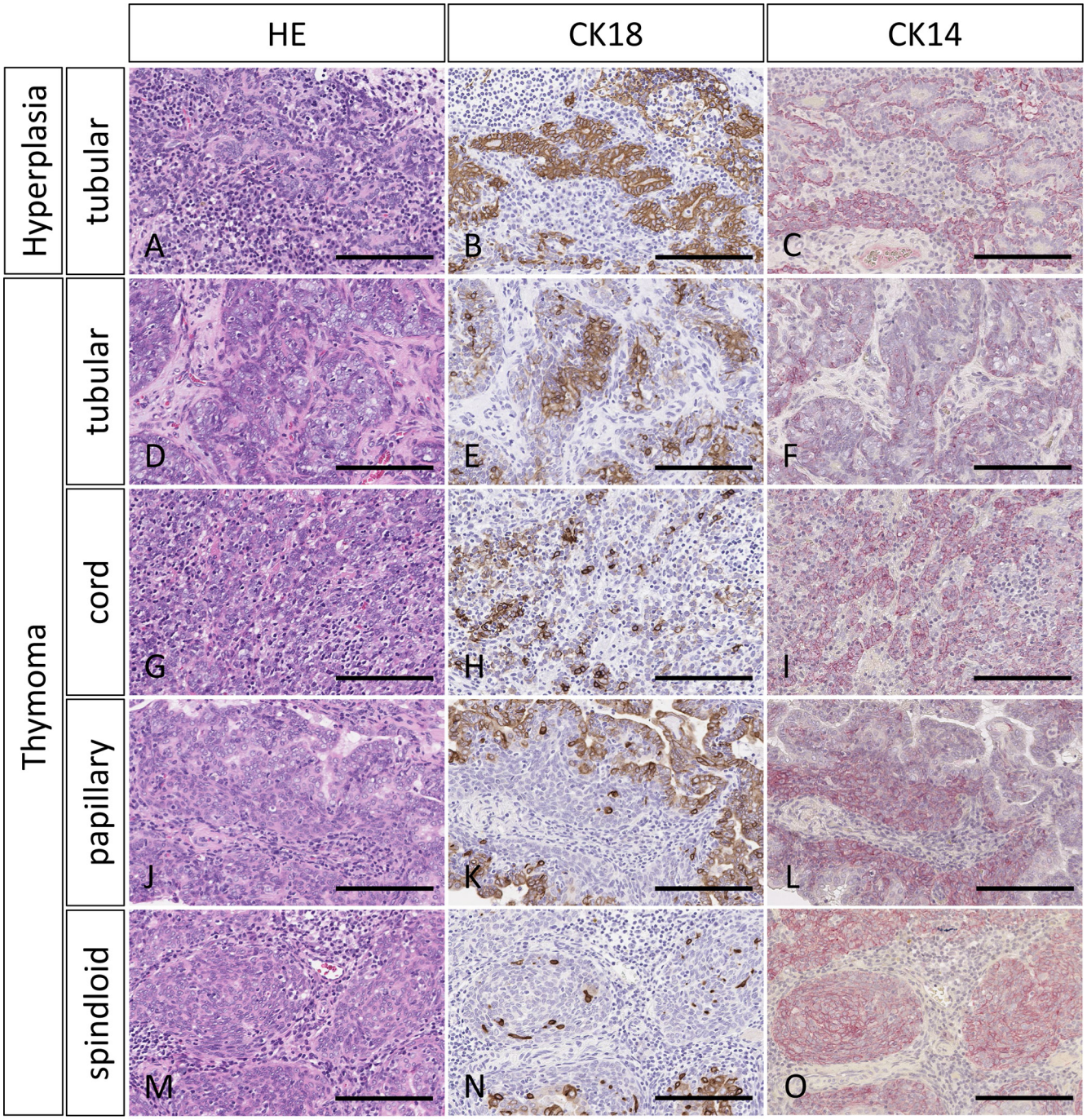

Fig. 2. A–C: TE hyperplasia, Case No. 3. D–F: Thymoma (tubular), Case No. 4. G–I: Thymoma (cord), Case No. 7. J–L: Thymoma (papillary), Case No. 6. M–O: Thymoma (spindloid), Case No. 6. The two-layer pattern of CKs is obvious in tubular structures, irregularly present in cord and papillary structures, not obvious in spindloid structures. A, D, G, J, and M: Hematoxylin and Eosin, Bar=60 µm. B, E, H, K, and N: Immunohistochemical stain for CK18. C, F, I, L, and O: Immunohistochemical stain for CK14. Bar=60 µm.

the spindloid areas, the two-layer pattern was not obvious, with round-to-oval TE were positive for CK14 and rarely positive for CK18 (Fig. 2N, 2O). Although CK14 is also used as a myoepithelial marker[9, 10], the outer cells in the present cases reacted negatively for α-SMA; indicating that they are mostly likely TE rather than myoepithelial cells. PAS staining revealed that a two-layered TE was present inside the basement membrane (BM) of the tubular structures in both the hyperplasia and thymomas (Fig. 1B, 1D). Additionally, the tubular lumens in TE hyperplasia were mostly filled with PAS-positive material (Fig. 1B), occasionally observed in the lumen of the tubular structures in thymomas (Fig. 1D). The BM was irregularly and/or discontinuously stained for PAS in the cord, papillary (Fig. 1F), and spindloid structures

of thymomas.

In Case No. 5, where thymoma exhibited tubular and cord structures, image recognition and synthesis using HALO® revealed two distinct color-coding of CK expressions can be observed in the part forming the lumen, in the cord structure, CK18 was scattered within the cord of CK14. Few CK14/18 double-positive cells were observed in the cord structure and outer layer of the tubular structure (Fig. 3).

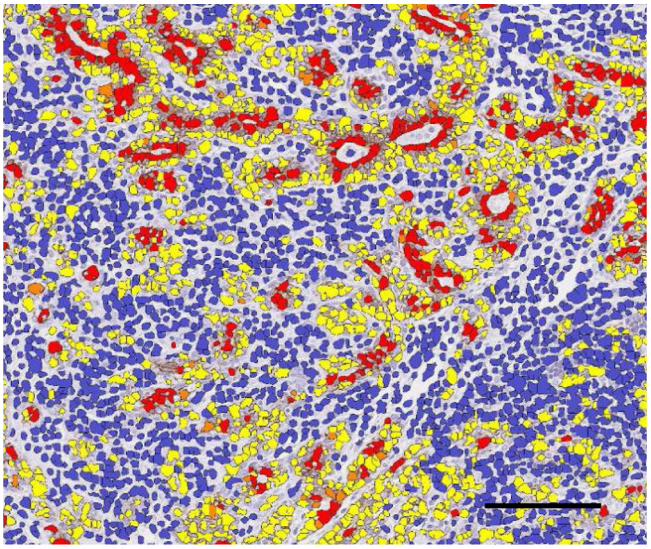

Fig. 3. Digital synthesized image by HALO® in case No. 5 (thymoma). The two-layer pattern is recognized and synthesized on one section by HALO®. CK18, CK14, and both positive areas are visualized in red, yellow, and orange, respectively. Negative areas are shown in blue. CK expression is color-coded in two distinct colors in most cells forming tubular or cord structures, although few double-positive cells for CK14/18 are observed. Bar=100 μm.

In the present study, we investigated the presence of a two-layer pattern of TE characterized by inner and outer epithelial layers, each expressing a different type of CK, which was particularly evident in the tubular structures of TE hyperplasia and thymomas in F334 rats. To our knowledge, this is the first study to elucidate this two-layer pattern using immunohistochemistry in TE hyperplasia and thymoma in F344 rats. This layered pattern of the two types of epithelia tends to be maintained even when the growth structure changes from tubular to cord and papillary. While the relationship between TE hyperplasia and thymomas has not been clearly defined[5], our results suggest that TE hyperplasia may develop into thymomas. The two-layered tubular structures in thymomas were similar to those in hyperplasia, including the immunohistochemical CK expression. We previously reported that hyperplasia and thymomas in WH rats had a cortex-like lymphocyte-rich area and a medullary differentiation area[3], showing morphologically and immunohistochemically similarities. This indicates that lesion size could be the most important characteristic for distinguishing between hyperplasia and thymomas in laboratory rats[3, 4]. Furthermore, considering the irregularity and/or discontinuity of the BM in the cord, papillary, and spindloid structures, the tubular structure would be a highly differentiated tumor, and the degree of differentiation potentially decreasing as progresses from tubular to cord, papillary, and spindloid structures. Human thymomas are subdivided based on their morphological and immunohistochemical criteria[11, 12]. However, in the human classification of thymomas, there are no descriptions of morphological and/or immunohistochemical descriptions for tubular structures consisting of an inner layer of cuboidal TE surrounded by an outer layer of round-to-oval TE in thymomas.

TE hyperplasia is considered to increase the number of tubules and cords, likely derived from branchial remnants[1]. Branchial remnants are derived from pharyngeal pouches during embryonic development and may persist in the parathyroid gland. The thymus develops from the third pharyngeal pouch during embryonic development, which forms the primordia of the thymus and parathyroid organs[1, 13]. The proximity of the thymus and branchial remnants during the embryonic development may be associated with the structures of the proliferative inner and outer TE. This origin is plausible, because the thymic ducts, which often persist in the thymus of laboratory monkeys and dogs, sometimes exhibit a two layered cellular pattern under detailed observation (Supplementary Fig. 1) and frequently contain proteinaceous material in the lumen. PAS-positive materials in the lumen of the tubular structure in rat thymomas have been described as homogenous eosinophilic materials in the previous reports[2, 5]. Accordingly, typical types of TE hyperplasia and thymomas in F344 rats may originate from branchial remnants.

The tubular structures of the TE are commonly observed in the medulla of atrophic thymus in aging rats, regardless of the strain, with a two-layer pattern observed in these structures (data not shown). It remains unclear whether these tubular structures originally existed within the thymic medulla and became more prominent as the thymus atrophied.

In conclusion, our study highlights the utility of CK14 and CK18 in distinguishing between the two-layered epithelial growth pattern in TE hyperplasia and epithelial-type thymomas in F344 rats. The differential CK expression observed between cortical and medullary TE in WH rats corresponds to the distinction between the inner and outer two cell layers in thymic hyperplasia and tumors in F344 rats, likely originating from branchial remnants.

Funding: The authors received no financial support for the research, authorship, or publication of this article.

Disclosure of Potential Conflicts of Interest: The authors declare no potential conflicts of interest with respect to the research, authorship, and/or publication of this article.

Acknowledgments: We gratefully acknowledge Ms. Kanae Tamatsukuri and Mr. James Harada for their assistance with language editing.

References

1. Willard-Mack CL, Elmore SA, Hall WC, Harleman J, Kuper CF, Losco P, Rehg JE, Rühl-Fehlert C, Ward JM, Weinstock D, Bradley A, Hosokawa S, Pearse G, Mahler BW, Herbert RA, and Keenan CM. Nonproliferative and proliferative lesions of the rat and mouse hematolymphoid system. Toxicol Pathol. **47**: 665–783. 2019. [Medline] [CrossRef]
2. Pearse G. Histopathology of the thymus. Toxicol Pathol. **34**: 515–547. 2006. [Medline] [CrossRef]
3. Tomonari Y, Sato J, Kurotaki T, Wako Y, Kanno T, and Tsuchitani M. Thymomas and associated hyperplastic lesions in Wistar Hannover rats. Toxicol Pathol. **47**: 129–137. 2019. [Medline] [CrossRef]
4. Tomonari Y, Sato J, Yamada N, Kurotaki T, Doi T, Kanno T, and Tsuchitani M. Immunohistochemical characteristics of thymomas and hyperplastic lesions in Wistar Hannover rats. Toxicol Pathol. **48**: 649–655. 2020. [Medline] [CrossRef]
5. Rebelatto MC. Thymus, spleen, lymph nodes, and thymus, Immune system. In: Boorman's Pathology of the Rat Reference and Atlas, 2nd ed. AW Suttie, JR Leininger, and AE Bradley (eds). Academic Press, London. 485–491. 2018.
6. Moore RR, Nagai H, Miller RA, Hardisty JF, Allison N, Shockley KR, and Malarkey DE. Comparative incidences and biological outcomes for thymoma in various rat strains in National Toxicology Program studies. Toxicol Pathol. **47**: 833–841. 2019. [Medline] [CrossRef]
7. Moroki T, Matsuo S, Hatakeyama H, Hayashi S, Matsumoto I, Suzuki S, Kotera T, Kumagai K, and Ozaki K. Databases for technical aspects of immunohistochemistry: 2021 update. J Toxicol Pathol. **34**: 161–180. 2021. [Medline] [CrossRef]
8. Janardhan KS, Jensen H, Clayton NP, and Herbert RA. Immunohistochemistry in investigative and toxicologic pathology. Toxicol Pathol. **46**: 488–510. 2018. [Medline] [CrossRef]
9. Duivenvoorden HM, Spurling A, O'Toole SA, and Parker BS. Discriminating the earliest stages of mammary carcinoma using myoepithelial and proliferative markers. PLoS One. **13**: e0201370. 2018. [Medline] [CrossRef]
10. Ogawa Y. Immunocytochemistry of myoepithelial cells in the salivary glands. Prog Histochem Cytochem. **38**: 343–426. 2003. [Medline] [CrossRef]
11. Marx A, Ströbel P, Badve SS, Chalabreysse L, Chan JK, Chen G, de Leval L, Detterbeck F, Girard N, Huang J, Kurrer MO, Lauriola L, Marino M, Matsuno Y, Molina TJ, Mukai K, Nicholson AG, Nonaka D, Rieker R, Rosai J, Ruffini E, and Travis WD. ITMIG consensus statement on the use of the WHO histological classification of thymoma and thymic carcinoma: refined definitions, histological criteria, and reporting. J Thorac Oncol. **9**: 596–611. 2014. [Medline] [CrossRef]
12. Kuo T. Cytokeratin profiles of the thymus and thymomas: histogenetic correlations and proposal for a histological classification of thymomas. Histopathology. **36**: 403–414. 2000. [Medline] [CrossRef]
13. Mense MG, and Rosol TJ. Parathyroid. In: Boorman's Pathology of the Rat Reference and Atlas, 2nd ed. AW Suttie, JR Leininger, and AE Bradley (eds). Academic Press, London. 687–693. 2018.